Article

Microbial Incorporation of ^{13}C-Labeled Acetate at the Field Scale: Detection of Microbes Responsible for Reduction of U(VI)

Yun-Juan Chang, Philip E. Long, Roland Geyer, Aaron D. Peacock, Charles T. Resch, Kerry Sublette, Susan Pfiffner, Amanda Smithgall, Robert T. Anderson, Helen A. Vrionis, John R. Stephen, Richard Dayvault, Irene Ortiz-Bernad, Derek R. Lovley, and David C. White

Environ. Sci. Technol., **2005**, 39 (23), 9039-9048 • DOI: 10.1021/es051218u

Environ. Sci. Technol. **2005**, *39,* 9039−9048

Microbial Incorporation of ^{13}C-Labeled Acetate at the Field Scale: Detection of Microbes Responsible for Reduction of U(VI)

YUN-JUAN CHANG,*,† PHILIP E. LONG,‡ ROLAND GEYER,†,§ AARON D. PEACOCK,† CHARLES T. RESCH,‡ KERRY SUBLETTE,‖ SUSAN PFIFFNER,† AMANDA SMITHGALL,† ROBERT T. ANDERSON,⊥,# HELEN A. VRIONIS,⊥ JOHN R.STEPHEN,▽ RICHARD DAYVAULT,× IRENE ORTIZ-BERNAD,⊥ DEREK R. LOVLEY,⊥ AND DAVID C. WHITE†

University of Tennessee, Knoxville, Tennessee, Environmental Technology, Pacific Northwest National Laboratory, Richland, Washington, Environmental Microbiology, UFZ Centre for Environmental Research Leipzig-Halle, Permoser Strasse 15, 04318 Leipzig, Germany, Center for Applied Biogeosciences, University of Tulsa, Tulsa, Oklahoma, Department of Microbiology, University of Massachusetts, Amherst, Massachusetts, Australian Genome Research Facility Ltd., Plant Genomics Centre, PMB1 Glen Osmond, SA 5064, Australia, S.M. Stoller Corporation, Lafayette, Colorado

A field-scale acetate amendment experiment was performed in a contaminated aquifer at Old Rifle, CO to stimulate in situ microbial reduction of U(VI) in groundwater. To evaluate the microorganisms responsible for microbial uranium reduction during the experiment, ^{13}C-labeled acetate was introduced into well bores via bio-traps containing porous activated carbon beads (Bio-Sep). Incorporation of the ^{13}C from labeled acetate into cellular DNA and phospholipid fatty acid (PLFA) biomarkers was analyzed in parallel with geochemical parameters. An enrichment of active *δ-proteobacteria* was demonstrated in downgradient monitoring wells: *Geobacter* dominated in wells closer to the acetate injection gallery, while various sulfate reducers were prominent in different downgradient wells. These results were consistent with the geochemical evidence of Fe(III), U(VI), and SO_4^{2-} reduction. PLFA profiling of bio-traps suspended in the monitoring wells also showed the incorporation of ^{13}C into bacterial cellular lipids. Community composition of downgradient monitoring wells based on quinone and PLFA profiling was in general agreement with the ^{13}C-DNA result. The direct application of ^{13}C label to biosystems, coupled with DNA and PLFA analysis, which combined detailed taxonomic description with a quantitative measure of metabolic diversity, allowed identification of the metabolically active portion of the microbial community during reduction of U(VI).

Introduction

A major challenge in microbial ecology and biogeochemistry is to relate observed biogeochemical processes to the associated bacterial populations, which is particularly difficult at the field scale. Identification of relevant bacterial populations has been traditionally achieved by enrichment and cultivation techniques. Since more than 99% of natural microorganisms are not culturable by standard cultivation techniques, alternative methods were developed to describe the community composition. One approach that revolutionized our understanding of microbial diversity was the use of rRNA-based molecular phylogenetic techniques (*1, 2*). Phospholipid fatty acid (PLFA) analysis is another powerful molecular tool that has been proven very useful in characterizing the microbial communities (*3*), and in monitoring changes in response to environmental contamination (*4, 5*).

Although application of the above molecular methods has provided considerable information regarding the microbial populations in a variety of environments, these approaches have not provided direct information on the active communities associated with specific environmental processes. The DNA-based phylogenetic analyses reveal the presence of sequences, including those originated from nonviable and/or nonactive organisms. PLFA measures viable community, but cannot differentiate active organisms from dormant species. Only within the past few years has the coupling of stable isotope probing (SIP) with DNA (*6, 7*) or PLFA (*8*) analyses been explored. Microorganisms that utilize ^{13}C-labeled compound often incorporate the label into their macromolecules (lipids, nucleic acids, amino acids, etc.), thus providing direct evidence of their active involvement in specific activities. Despite the success of SIP-based studies for the analysis of microbial populations (*9, 10*), this approach has seldom been applied at the field scale due to concerns regarding cost and dilution of the ^{13}C-labeled substrate within an unconfined natural environment. We addressed this challenge by trapping ^{13}C label within Bio-Sep beads (University of Tulsa, Tulsa, OK), which have been shown to be rapidly colonized in a variety of aqueous environments, and subsequently yielding information regarding viable biomass and community structure of the subsurface microbial communities (*11*−*13*). Potential remediation amendments can be incorporated into the Bio-Sep beads during fabrication by entrapment (such as ^{13}C-acetate) or post-fabrication by adsorption (such as volatile hydrocarbons) onto the powered activated carbon (PAC) component of the beads, thus providing slow releasing and undiluted substrate at the points-of-interest at largely reduced costs compared to direct injection at field.

Uranium contamination is a serious problem worldwide. Natural and accelerated attenuation as a decontamination strategy for uranium-contaminated subsurface has been widely accepted over the past two decades as a cost-effective method (*14*−*16*). Previous studies indicated that specific nutrient additions in the contaminated zone could stimulate the growth of indigenous organisms capable of enzymatically reducing uranium and achieving the goal of immobilizing polluting heavy metals at the site *(17, 18)*. It was hypothesized that the stimulated metal redox shifts are microbially driven

* Corresponding author e-mail: ychang1@utk.edu; fax: 865 974 7297; tel. 865 974 7792.
† University of Tennessee.
‡ Pacific Northwest National Laboratory.
§ UFZ Centre for Environmental Research Leipzig-Halle.
‖ University of Tulsa.
⊥ University of Massachusetts.
Currently at U.S. Department of Energy (SC-23.4).
▽ Australian Genome Research Facility Ltd.
× S.M. Stoller Corporation.

10.1021/es051218u CCC: $30.25
Published on Web 10/19/2005

and the rate of metal reduction is governed by microbial biomass. Thus microorganisms in natural environments that possess the ability to enzymatically reduce U(VI) to insoluble U(IV) play important roles in uranium bioremediation. To optimize in situ biostimulation and uranium bioremediation strategies, it is important to identify the indigenous organisms that are actively involved in the bioremediation process, and to link the bio-geochemical functions to the identity of those organisms.

In this study, we report the detection of microbial incorporation of ^{13}C-labeled carbon from acetate-amended bio-traps at the Old Rifle field and the association between stimulated uranium reduction and microbes responsible for the activity. The objectives of the work reported here were to (i) determine the feasibility of detecting ^{13}C incorporation in DNA/PLFA biomarkers derived from suspended bio-trap samplers; (ii) examine the biogeochemical functions and active microbial populations stimulated by acetate injection; and (iii) link the microbial identity to geochemical functions. Bacterial community structure was analyzed by denaturing gradient gel electrophoresis (DGGE) analysis of ^{13}C-labeled 16S rRNA gene fragments generated by PCR amplification with universal bacterial primers. Viable biomass, structure, and respiratory state of the community were examined using phospholipid fatty acid and quinone analysis. Our results demonstrated the effectiveness of using ^{13}C labeling to link the microbial populations to biostimulation and uranium bioreduction by focusing on the active members of the community. To our knowledge, this is the first attempt to follow uranium bioreduction using ^{13}C-DNA biomarkers directly at the field scale in a natural contaminated subsurface environment.

Materials and Methods

Site Description. The test plot sits within a uranium-contaminated aquifer, which is located at the Old Rifle site, a former uranium ore processing facility in Rifle, CO. The site is now a part of the Uranium Mill Tailings Remedial Action (UMTRA) program of the U.S. Department of Energy (*19*).

Uranium contamination in groundwater within the plot ranged from 210 μg L^{-1} to 433 μg L^{-1}, exceeding the UMTRA maximum contamination limit of 42.85 μg L^{-1}. Prior to initiation of this study, the site had been under natural groundwater flow without acetate amendment for 8 months. Groundwater analysis over this time showed no significant increase in dissolved oxygen (DO) after cessation of a previous biostimulation experiment at the site (*17*). Trace levels of nitrate (3.1−18.6 mg L^{-1}) were observed in some of the monitoring wells, while sulfate concentrations ranged from 730 to 912 mg L^{-1}.

An injection gallery positioned perpendicular to groundwater flow was installed to inject acetate into the subsurface. To evaluate stimulated changes, downgradient monitoring wells were installed at distances of 3.7 m (M-03), 7.3 m (M-08), and 14.6 m (M-13) from the injection gallery. A monitoring well was also placed 3.7 m (B-02) upstream of the injection gallery to serve as the background well (See Figure S1 in the Supporting Information, and ref *17*).

In this experiment, native groundwater amended with nonlabeled sodium acetate was prepared and injected into the subsurface at an appropriate concentration and rate to produce ~10 mM sodium acetate within the aquifer. Detailed site descriptions and test plot design for this experiment have been described elsewhere (*19*).

Groundwater Sample Acquisition. Acetate injection into the aquifer began on June 27, 2003, and was continuous over a 3.5 month period until mid-October. Groundwater samples were systematically collected at regular intervals from all background and downgradient monitoring wells during the experiment. The pH, dissolved oxygen (DO), sulfide, ferrous iron (II), and the redox potential (E_h) were determined from groundwater pumped using a portable peristaltic pump (ColePalmer Instrument Co.) from 5.4 m below top of casing. All wells were purged (about 12 L) until groundwater parameters stabilized. Sulfate, nitrate, acetate, and uranium (VI) concentrations were determined from groundwater samples at discrete vertical zones of ~5 m and ~6 m depths using multi-level passive diffusion samplers (MLS). The MLS contained dialysis cells fitted with 0.2-μm permeable membranes at both ends enabling exchange with surrounding groundwater. After recovery of the MLS dialysis cells, the equilibrated groundwater was filtered (0.2 μm, Teflon, AllTech Associates) and placed into 15-mL polystyrene conical Falcon tubes. The water samples were then shipped to the laboratory via overnight courier and stored at 4 °C prior to analysis. After sampling, the MLS dialysis cells were washed at least twice with distilled water and then completely refilled with distilled water and placed back into their sampling positions on the MLS well insert. The MLS insert was then slowly positioned back into the monitoring well.

Bead Amendment and Bio-Trap Sampling. Bio-Sep beads amended with ^{13}C-sodium acetate were fabricated by suspending powdered ^{13}C-sodium acetate (99%, ISOTEC) and powdered activated carbon (PAC) in a solution of Nomex in dimethylacetamide (DMAc). This suspension was then forced under pressure through a nozzle with droplets falling into an aqueous quenching solution. Beads, about 3−4 mm in diameter, were obtained with ^{13}C-sodium acetate and PAC uniformly distributed throughout the beads as determined by microscopic examination. The final composition of the beads was approximately 20−25% ^{13}C-sodium acetate, 50−55% PAC, and the balance Nomex by weight. The porosity was comparable to that of standard Bio-Sep beads (about 74%).

Bio-traps consisted of an 11.4-cm piece of perforated PFA tubing (1.25-cm o.d., 0.95-cm i.d. with 2.3-mm holes) closed at each end with glass wool and nylon cable ties. Prior to bio-trap assembly all plastic parts were rinsed with methanol. Glasswool and standard Bio-Sep beads were heated to 300 °C for 4 h.

The control bio-traps are the normal Bio-Sep beads samplers or standard bio-traps, containing about 100 standard Bio-Sep beads. The iron bio-traps are prepared as standard bio-traps with a total of 10−20 mg ferrihydrite added to the bottom and middle of the traps, respectively. These iron bio-traps were included in this test to examine possible enrichment effect for iron/uranium reducers, also to serve as replication.

Both control and iron traps may be constructed with ^{13}C-acetate amendment, which was done by packing 50 Bio-Sep beads amended with ^{13}C-sodium acetate and 50 standard nonamended beads. The two types of beads were uniformly distributed within the bio-traps. In water the amended beads can act as a slow-release source of labeled electron donor within the bio-traps (*13*).

The bio-traps equipped with multi-level samplers (MLS) were suspended down-well at depths of ~5 m and ~6 m, respectively. At ~5 m depth, the control and iron traps were both amended with ^{13}C-acetate for the purpose of identifying active microbial populations involved in the stimulated process in the subsurface. The traps with ^{13}C amendment were deployed on 8/7/03 and incubated for around 30 days as described by Peacock et al. (*12*). The traps for quinone analysis were deployed earlier at three different dates and recovered on 6/26/03, 7/24/03, and 8/7/03 respectively, after 30 day incubation. Those traps were retrieved from wells B-02, M-03, M-08, and M-13 (Figure S1). Once recovered, the bio-trap samplers were frozen onsite with dry ice, shipped

to the CBA laboratory, and stored at −80 °C prior to lipid and DNA analysis.

Geochemical Measurement. Acetate was measured on a Hewlett-Packard series 1100 high-pressure liquid chromatograph (Agilent technologies, Albany, NY) using a fast-acid analysis column (Bio-Rad, Hercules, CA) with 0.5 M H_2SO_4 eluent and absorbance detection (210 nm). Sulfate and nitrate were determined as components of a suite of anions analyzed using ion chromatography (Dionex model DX-300) according to McKinley et al. (*20*). Uranium (VI) concentrations were determined using a kinetic phosphorescence analyzer (model KPA-11, Chemchek Instruments, Inc.) as described by McKinley, et al. (*21*). The detection limit was 0.3 μg L^{-1}. The pH, DO, and E_h were determined during well purging using a calibrated flow-through DS3 Data Sonde instrument (HACH Environmental, Inc). The sonde was calibrated against standard buffers for pH, against the atmosphere for oxygen, and against Zobells Solution (Ricca Chemical Co.) for E_h. Stable DO values typically occurred prior to completion of well purging; the minimum observed concentration was taken as the in situ value. Sulfide and ferrous iron were determined in the field on unfiltered samples using a portable spectrophotometer with colormetric methods (HACH Environmental, Inc.).

DNA Extraction and CsCl Gradient Separation. Nucleic acids were extracted directly from bio-trap beads using a FastDNA Spin Kit (for soil, BIO101 Inc., La Jolla, CA) following manufacturer's instruction. CsCl gradient separation was performed as described in Chang (*22*). Briefly, 1 g of CsCl was added to 1 mL of DNA solution in TE buffer containing 10 μL of ethidium bromide (10 mg mL^{-1}), which was then transferred to a polyallomer Bell-top ultracentrifuge tube (11 × 32 mm, Beckman). DNA fractions were resolved following centrifugation at 70 000 rpm using a Beckman TL-100.2 rotor (TL-100 Beckman Ultracentrifuge) for 22 h at 20 °C in a CsCl density gradient and visualized with UV light (365 nm). DNA from the "heavy" (^{13}C-labeled) fraction was withdrawn gently from the gradients using a 1-mL syringe and hypodermic needle (18 gauge). Care was taken during collection of the ^{13}C DNA fraction to avoid co-extraction of the "light" ^{12}C-DNA fraction.

The ^{12}C and ^{13}C DNA standards were extracted from *E. coli* grown overnight on basic cultivation medium with addition of normal D-glucose or D-glucose−^{13}C (99 at. % ^{13}C, Sigma-Aldrich), respectively. A mixture of 10 μg of ^{12}C- and ^{13}C-DNA standards was run as a control in each CsCl ultra centrifugation separation. In a situation where ^{13}C-DNA band was not visible, the standard control tube was aligned with the sample tube and ^{13}C-DNA was withdrawn from the position where the standard indicated.

Ethidium bromide was removed from the DNA by extraction using an equal volume of *n*-butanol saturated with deionized water. Following 3 butanol extractions, the DNA was dialyzed against a large volume of sterilized deionized water using Tube-O-Dialyzer (Geno Technology Inc., St. Louis, MO) and then used for PCR.

PCR-DGGE and Sequence Analysis. PCR amplification of the 16S rDNA fragments, obtained from either total genomic DNA extract, or from the "heavy" ^{13}C-labeled fraction, was performed as described by Muyzer et al. (*23*). DGGE was performed using a D-Code 16/16 cm gel system (BioRad, Hercules, CA) as described in Chang et al. (*24*). Prominent bands formed by ^{13}C-labeled DNA were excised and sequenced. Sequences were first identified by use of the BLASTN site facility (www.ncbi.nlm.nih.gov, the National Center for Biotechnology Information) and then assembled using SeqPup Version 0.6 (*25*). Both ARB package (www.mikro.biologie.tu-muenchen.de) and RDP-on line analysis of the Ribosomal Database Project (*26*) were used for sequence alignment. Phylogenetic algorithms (DNA-DIST, NEIGHBOR, and SEQBOOT) were operated within the ARB software environment (*27*). Partial 16S rDNA sequences recovered from this study were submitted to GenBank with accession numbers AY994914−AY994977.

Phospholipid Fatty Acid (PLFA) Analysis and Isotope Ratio Mass Spectrometry (IRMS). The analysis of PLFA was performed using previously reported precautions (*3*). In brief, Bio-Sep beads were extracted with the single-phase chloroform−methanol−buffer system of Bligh and Dyer (*28*), as modified by White et al. (*29*). The total lipid extract was fractionated into neutral lipids, glycolipids, and polar lipids by silicic acid column chromatography. The polar lipids were transesterified to the fatty acid methyl esters (FAMEs) by a mild alkaline methanolysis, with the method of Mayberry and Lane (*30*) to protect cyclopropane PLFA and release plasmalogen ethers as dimethylacetals. The FAMEs were analyzed by gas chromatography/mass spectroscopy using an Agilent 6890 series gas chromatograph interfaced to an Agilent 5973 mass selective detector with a 50-m nonpolar column (0.2 mm i.d., 0.11 μm film thickness). The temperature program for analysis was 100 °C initial temperature, 10 °C min^{-1} to 150 °C for a minute, and 3 °C min^{-1} to 282 °C for 5 min, with injector temperature at 270 °C and detector at 290 °C.

The measurements of stable carbon isotope ratios (^{13}C/^{12}C) were performed on a Finnigan Delta Plus isotope ratio mass spectrometer (Thermo, Austin, TX) coupled to a GC-III Combustion interface and an Agilent 6890 gas chromatograph (Palo Alto, CA). The fatty acid methyl esters were separated on an HP-1 column (dimensions 50 m × 200 μm) with constant pressure at 43.7 psi. The oven (column) temperature was programmed from 60 to 150 °C at 10 °C min^{-1}, then to 312 °C at 3 °C min^{-1}.

Respiratory Quinone Analysis. After fractionation on silicic acid columns, the neutral lipid fraction of the Bligh and Dyer (*28*) extract was examined for quinone classes. The respiratory ubiquinone and menaquinone isoprenologues were determined by high-performance liquid chromatography/atmospheric pressure chemical ionization tandem mass spectrometry (HPLC/APCI/MS/MS) (*31*).

Statistics. The regression and correlation analysis between geochemical variables and PLFA biomarkers were performed using the statistical package JMP Version 5.1.2 for Windows (JMP, SAS Institute. Inc., Gary, NC).

Results and Discussion

The experimental approach combined a large-scale injection of nonlabeled acetate in an injection gallery with the downwell deployment of labeled acetate bio-traps during active biostimulation and bioreduction. Consumption of acetate drove the subsurface environment to anaerobic condition. Anaerobic microorganisms typically use additional electron acceptors in the following order of preference: nitrate, ferric iron, sulfate, and finally carbon dioxide (*32*). Evaluation of the distribution of these electron acceptors provides evidence of where and under what condition uranium bioreduction may occur.

Stimulated Anaerobic Respiration. Groundwater chemistry showed substantial differences between the background and downgradient monitoring wells. A biostimulatory effect resulting from acetate injection was clearly demonstrated.

About 20 days after injection, acetate reached all downgradient monitoring wells (Figure 1A), where the redox potentials underwent intense reduction for a period of approximately 1+ month after acetate injection (Figure 1B). This indicated a lack of oxygen and the development of reducing condition. By day 40 after injection, the redox potentials of all downgradient monitoring wells were reduced to a value of less than 0 mV, which spanned the ^{13}C-bio-trap incubation duration. Without acetate addition, a more

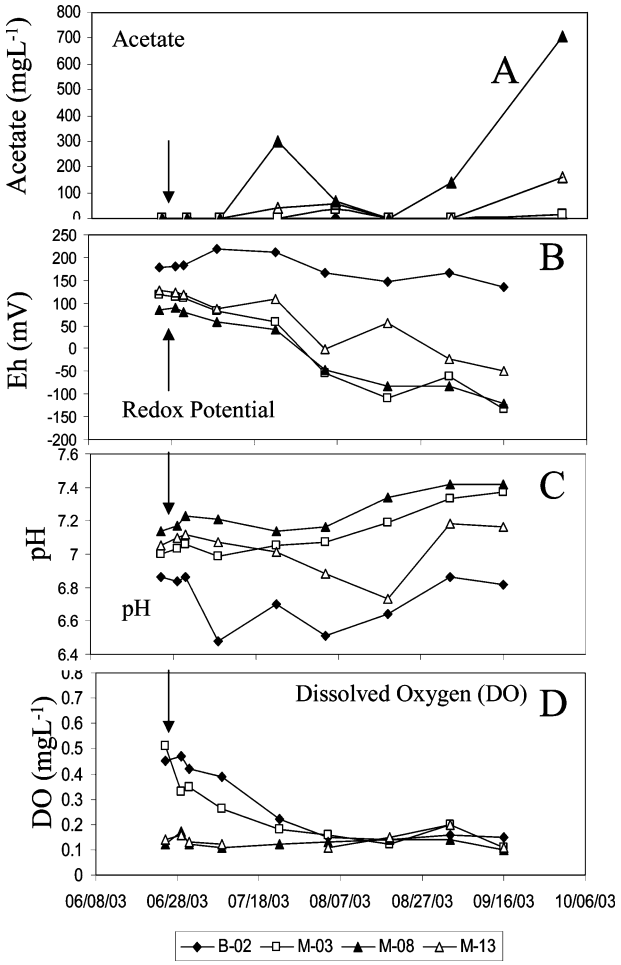

FIGURE 1. Change in concentrations of acetate (A), redox potential (B), pH (C), and dissolved oxygen (D) in Rifle groundwater during acetate biostimulation experiment. All data points are the means of triplicate measurements. Arrow indicates start of acetate injection.

oxidized condition was maintained in the background well throughout the experiment (Figure 1B). The pH values in all downgradient monitoring wells were moderately elevated compared with background well (Figure 1C), consistent with alkalinity resulting from HCO_3^- generated by acetate oxidation. Dissolved oxygen (DO) within the treatment plot remained at approximately 0.13 ± 0.03 mg L^{-1} ($n = 12$) after an initial drop and was slightly lower than that in the background well (Figure 1D).

The proportion of aerobically respiring organisms indicated by the ubiquinone/menaquinone ratio (UQn/MKn) also suggested a transition from aerobic to anaerobic respiration after acetate injection, with UQn/MKn dropping below 1 in downgradient monitoring wells roughly one month after injection (Table 1); this suggests anaerobic condition with a past history of oxygen availability (*31*, *33*). The ratio of UQn/MKn in background wells remained well above 1, indicating aerobic or partial microaerophilic condition in the presence of gram-negative bacteria (*31*, *33*−*35*). Clearly, aerobic or microaerophilic conditions in the original subsurface groundwater changed to anaerobic as injected acetate was microbially metabolized.

Reducing Activities and Potential U Reducers. Fe(III) reduction was directly evidenced by the rapid accumulation of soluble Fe(II) (Figure 2A). Sulfate reduction was supported by an increase of sulfide concurrent to decrease of sulfate (Figure 2B and C), which significantly correlated to each other in all three downgradient wells (see Figure S2 in the Supporting Information). Despite the production of soluble Fe(II) following the acetate application, dissolved ferrous iron concentrations eventually returned to preapplication levels or even lower. The decline in soluble Fe(II) was accompanied by a decrease in sulfide (Figure 2A and B), suggesting precipitation of both as iron sulfides. Well M-08 displayed the highest rate of sulfate reduction (Figure 2C), but the lowest iron reduction rate (Figure 2A).

Although the breakthrough of upstream U(VI) may have caused some U(VI) fluctuations observed in downgradient monitoring wells, uranium reduction was evidenced by a decrease in groundwater U(VI) concurrently with Fe(II) production in wells M-08 and M-13, or shortly after an increase of ferrous iron was observed within well M-03 (which reflects the heterogeneity of the environment).

Abiotic reduction of U(VI) by sulfide or Fe(II) are major pathways of uranium immobilization in a wide range of redox-stratified environments (*36, 37*). In this experiment, U(VI) reduction was initiated before sulfate reduction in most cases (Figure 2), and continued beyond the Fe(II) production phase, which supports the conclusion that uranium reduction in this experiment occurred via a direct enzymatic pathway.

Among all electron acceptors evaluated, sulfate was quantitatively dominant with an initial concentration of 850 $\pm$ 44 mg L^{-1}, while U(VI) initial concentration averaged 210 $\pm$ 80 μg L^{-1}. A significant correlation was demonstrated between decrease of redox potential and loss of sulfate in all three downgradient monitoring wells, with strongest correlation in well M-08 ($r^2 = 0.95$, $P < 0.0001$, Figure S2, Supporting Information), and the weakest correlation in well M-13 ($r^2 = 0.61$, $P = 0.0226$) (data not shown). This indicated that the observed reduction was largely caused by the oxidation of the acetate coupled to sulfate reduction and sulfate reduction was the overall driving force in altering the subsurface redox condition. The monitoring wells M-03 and M-08 were noticeably more reduced, perhaps due to their higher rate of metal and sulfate reduction following acetate metabolism (Figure 1B). Nitrate was consistently below the detection limit (<0.056 mg L^{-1}) in all wells until two months (~52 days) after the initiation of injection (data not shown), and therefore nitrate posed little concern in this study.

The uranium concentration in well M-08 decreased rapidly and the resulting low concentration of uranium U(VI) was generally maintained. But uranium concentration in well M-13 showed significant fluctuations (Figure 2D). This suggests that bio-traps suspended in well M-08 would more likely reflect uranium-reducing populations. Coincidently, sulfate reduction showed the highest rate in well M-08, which raises the question of the role of SRBs in uranium reduction and maintenance.

A number of sulfate reducers within the δ-subdivision of the *proteobacteria* have been found to be able to reduce Fe(III) and U(VI) in pure culture (*38*−*41*). Barton et al. (*42*) reported that the sludge inoculum growing in the presence of higher concentrations of sulfate (3.0 g L^{-1}) accounted for greater levels of reduced U(IV) than at low levels of available sulfate (0.3 g L^{-1}). Furthermore, SRB cultures, both mixed and pure, have exhibited a faster rate of uranium reduction in the presence of sulfate and no lag time until the onset of uranium reduction in contrast to uranium alone (*43*). On the basis of observation in this study and previous reports, we hypothesize that sulfate-reducing organisms may reduce both U(VI) and sulfate in subsurface groundwater when it becomes anaerobic during bioremediation and when bioavailable Fe(III) is consumed by Fe-reduction. Sulfate-reducing bacteria my have also directly or indirectly maintained the reduced state of uranium in this study.

Analyses of ^{13}C Incorporation and Link Identity to Function. Down-well deployment of ^{13}C-amended bio-traps provides a convenient way to identify microbial populations active in subsurface, if the label is incorporated in DNA and

TABLE 1. Respective Ubiquinone to Menaquinone Ratio (UQn/MKn) and Quinone Class MK8 Mole Percent Detected from Bio-Traps Suspended in Both Background (B-02) and downgradient Monitoring Wells (M-03, M-08, and M-13)[a]

date collected	UQn/MKn ratio				MK8 (mol %)			
	B-02	M-03	M-08	M-13	B-02	M-03	M-08	M-13
				Control Bio-Traps				
06/26/03	6.45	MKn = 0	27.27	3.81	0	0	0	0
07/24/03	MKn = 0	23.24	1.39	2.88	0	4.1	28.4	17.6
08/07/03	9.47	1.79	1.16	0.67	0	24.3	34.3	47.4
				Iron Bio-Traps				
06/26/03	147	1.15	1.06	0.69	0.8	0.8	1.7	2
07/24/03	MKn = 0	9.25	0.57	ND	0	6.2	50.5	ND
08/07/03	MKn = 0	0.81	0.40	0.55	0	40.5	55.7	50.5

[a] ND=not determined, no data; MKn = 0, there was considerable amount of UQn detected, but not MKn.

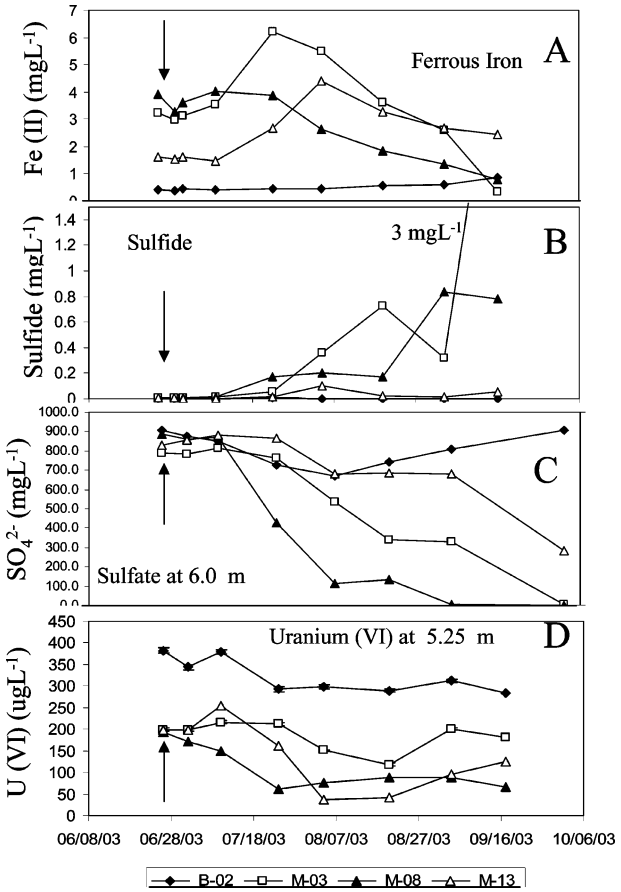

FIGURE 2. Iron reduction, sulfate reduction, and uranium reduction as measured by Fe(II) production (A), sulfide production (B) versus sulfate disappearance (C), and U(VI) disappearance (D), respectively. Arrow indicates start of acetate injection.

afterward extracted and amplified. Due to relatively low biomass obtained within the in situ experiment, the ^{13}C-DNA fraction was not clearly visible after CsCl gradient centrifugation and thus was withdrawn according to standard indication. Sufficient PCR products for DGGE analysis were obtained from all ^{13}C-DNA fractions extracted.

The banding pattern of amplified 16S rDNA revealed by DGGE analysis indicated a markedly different structure for the background well, while monitoring wells M-03 and M-08 shared most similarities (Figure 3). In wells M-03 and M-08, nearly all bacterial community members captured on bio-trap beads actively consumed ^{13}C-acetate. However, the PCR-DGGE migration pattern also showed that rDNA templates present in the "heavy" fraction (^{13}C-labeled) differed from the overall community, most noticeably in wells B-02 and

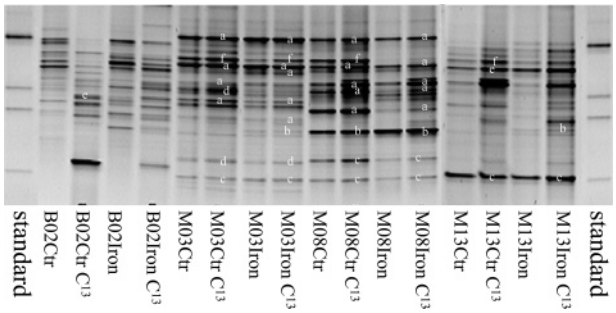

FIGURE 3. DGGE analysis of bacterial community recovered from bio-trap beads. Amplified 16S rDNAs were separated on a gradient of 20% to 65% denaturant. Iron denotes the iron bio-traps. Ctr. represents the standard control bio-trap. The ^{13}C-labeled community was compared with the community profile containing both ^{13}C and ^{12}C fractions (e.g., M08Iron C^{13} compared with M08Iron). Band label: (a) *Geobacter*, (b) *Pelobacter/Desulfuromonas*, (c) unclassified *δ-proteobacteria*, (d) *Desulfobacter* and its relatives, (e), (f) *Pseudomonas*. For more detailed designation information, refer to Figures 4 and 5.

M-13 (Figure 3), which is an important prerequisite for the correct interpretation of environmental SIP data. Strong enrichment of one type of sequence over another was not observed among bio-traps and iron traps.

Phylogenetic trees in Figures 4 and 5 show the major bacterial lineages labeled by the incorporation of the ^{13}C-acetate carbon, which are interpreted to be the active populations. The background wells displayed the highest level of diversity. Sequences retrieved include α-*proteobacteria,* *β-proteobacteria,* actinobacteria, and organisms belonging to the *Cytophaga-Bacteroides-Flexibacter* division (CBF phylum). Among them, *β-proteobacteria* (33%) and α-*proteobacteria* (44%) constitute the majority of the sequences, such as *Methylophilus, Hyphomicrobiaceae, etc.* (Figure 4). Wells of M-03 and M-08 exhibited a lower diversity and analysis of ^{13}C-16S rDNA sequences indicated a predominance of *δ-proteobacterial* phylotypes, represented by four clusters (Figure 5).

The (a)-cluster was the largest group containing 14 bacterial sequences belonging to *Geobacter*, ~93% of them were recovered from wells M-03 and M-08, where geochemistry demonstrated strong evidence for uranium reduction. All *Geobacter* bands remained strong in wells M-03 and M-08, but had disappeared from M-13 (Figures 3 and 4).

The exclusive recovery of ^{13}C-labeled *Geobacter* sequences from wells M-03 and M-08 indicates that those *Geobacter* conducting the acetate oxidation were quantitatively significant in the uranium bioreduction stimulated by acetate injection. Members of the *Geobacteraceae* family are well-known Fe(III) reducing organisms, have been isolated from many subsurface environments (*15*), and have previously

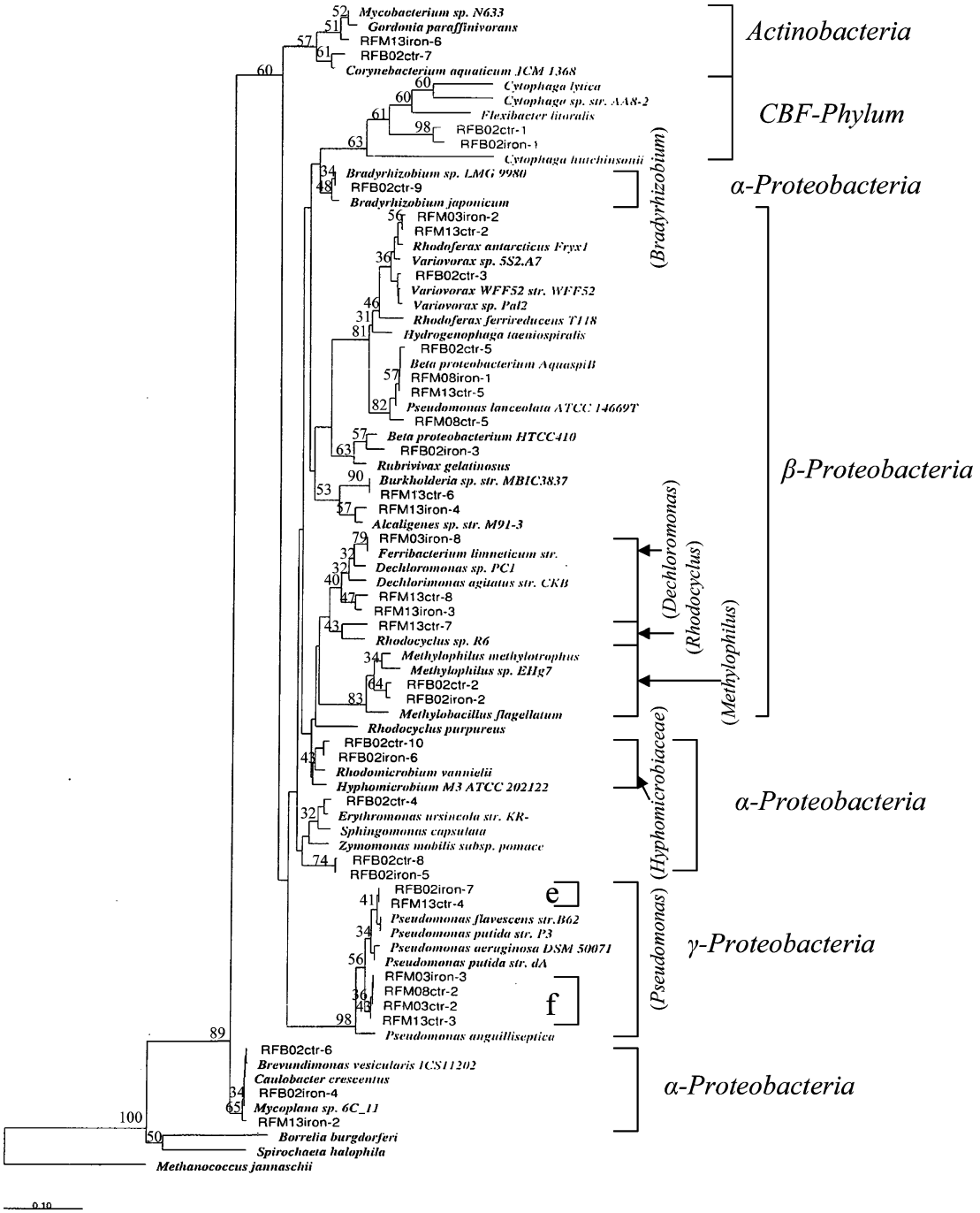

FIGURE 4. Neighbor-joining analysis of ^{13}C-labeled 16S rDNA sequences from excised DGGE bands, derived from this investigation. Relationships with reference organisms from bacterial genera other than *δ-proteobacteria*. Numbers on the tree refer to bootstrap values on 1000 replicates; only values above 30 are given. Scale bar represents 10% estimated change. Sequences prefixed "RF" were generated during this study. Nomenclature: The prefix ("RF") is followed by the well number (B-02, M-03, M-08, and M-13), then bead type (ctr = control, or iron) and at the end, band number from original DGGE gel image.

been reported to be associated with uranium reduction (*17*). Data presented in this study once again confirmed their association with uranium reduction. More importantly, this study demonstrated that the *Geobacter* are functionally and metabolically active during acetate-stimulated uranium reduction at the Old Rifle site.

The (b)-cluster included three sequences obtained from all downgradient monitoring wells, with higher relative abundance in well M-08. Comparative sequence analysis revealed that none of the (b)-sequences was identical to 16S rRNA sequences of cultured microorganisms. However they branched within the radiation of cultivated representatives of the *Pelobacter*/*Desulfuromonas* genera, and appeared evolutionally closer to the *Desulfuromonas* lineage than to *Pelobacter* group (Figure 5).

The (c)-cluster represented a novel linage so far described only by two environmental sequences. The sequences recovered within this cluster share ~96% identity with an uncultured *δ-proteobacterium* Fe_C-138 (AY752784), which was detected from an iron-reducing aquifer in the Banisveld landfill. It also shared 95% sequence identity with an uncultured iron-reducing bacterium (AY524550) detected from an iron (III)-reducing enrichment obtained from acidic subsurface sediments contaminated with U(VI) (*44*). Phylogenetic affiliation makes it likely that the source organisms are associated with *Pelobacter*/*Desulfuromonas* genera. Both

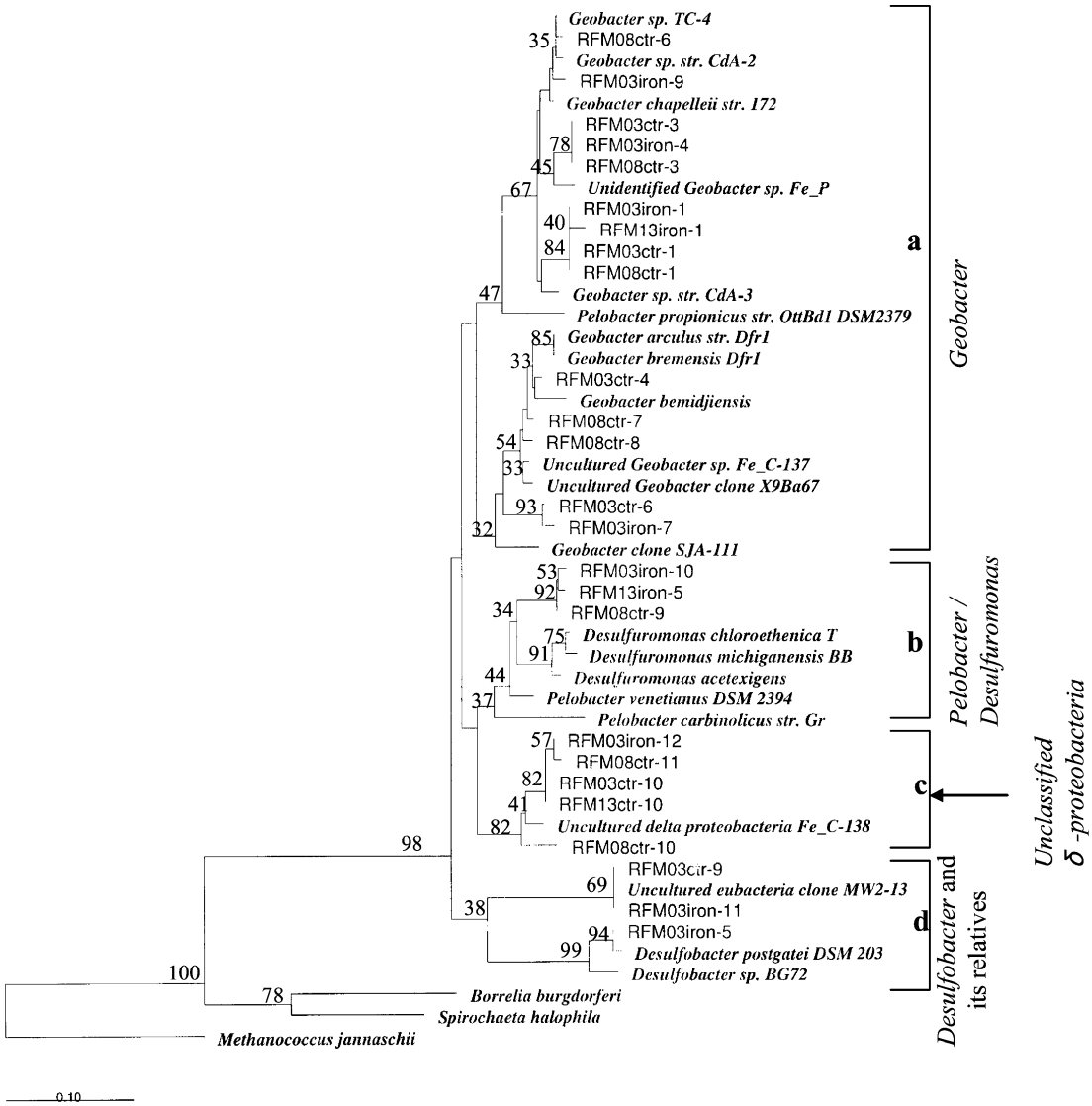

FIGURE 5. Neighbor-joining analysis of ^{13}C-labeled 16S rDNA sequences from excised DGGE bands. Relationships with reference organisms from *δ-proteobacteria,* obtained from RDP. Numbers on the tree refer to bootstrap values on 1000 replicates; only values above 30 are given. Scale bar represents 10% estimated change. Refer to Figure 4 caption for nomenclature.

Pelobacter/*Desulfuromonas* belong to the family of *Geobacteraceae*, and members are capable of both iron reduction and sulfate reduction.

For environmental rDNA sequences with no known cultivated representatives, any physiological interpretations must rely heavily on the environmental conditions of a sample from which the sequence was generated. On the basis of the groundwater chemistry, and the affiliation with other species, it is likely that organisms represented by the (b) and (c) cluster sequences are actively engaged in Fe(III)- and uranium-reducing activities and are also capable of sulfate reduction.

Previous in situ field experiments conducted at the Old Rifle site demonstrated that U(VI) reduction was less efficient under stimulated sulfate-reducing conditions than under Fe(III)-reducing conditions and either breakthrough of upstream U(VI) or possibly (but inconsistent with the reduced status of the system) reoxidation of U(IV) occurred during sulfate reduction period (*17*). Thus the ability of dissimilatory Fe(III)-reducing bacteria to reduce both Fe(III) and sulfate may bear advantages in the field uranium bioremediation. These organisms are likely to be present at the interface between sulfate- and Fe(III)-reducing zones in subsurface environments, and able to gain energy from oxidation of acetate with Fe(III) or U(VI) if and when Fe(III) or U(VI) get into a previously sulfate-reducing environment. This may provide additional explanation how reduced uranium was maintained in this experiment.

The (d)-cluster sequence was retrieved exclusively from well M-03, closest to the injection well, and represented by *Desulfobacter* and *Desulfobacter* relatives (Figure 5). It was expected that bioavailable Fe(III) or U(VI)would be first depleted in or very near the injection gallery, and sulfate reduction would then became a more competitive process. Under such conditions, *Desulfobacter* sp. have been shown to primarily and directly consume acetate (*45*). Furthermore, *Desulfobacter* is a well-known sulfate-reducing bacteria but no report has associated them with metal reduction. Therefore, the *Desufobacter* detected here was an active component of the community, but more likely involved in sulfate reduction rather than uranium reduction.

The ability of bacteria to use Fe(III) or U(VI) as a terminal electron acceptor is not limited to members of the *δ*-subdivision of *Proteobacteria.* Another prominent active sequence detected in downgradient wells M-03 and M-08 was a *Pseudomonas* (band f, Figure 3), which differed from the *Pseudomonas* sequence detected in the background well. *Pseudomonas* is known to be capable of reducing nitrate (*46*), nevertheless there was no significant nitrate concentra-

TABLE 2. Summary of Major Community Shifts Indicated by PLFA Analysis[a]

Bio-trap samples	At ~5 m Depth				At ~6 m Depth			
	B-02	M-03	M-08	M-13	B-02	M-03	M-08	M-13
				biomass (pmol/bead)				
control trap	0	5.93	105.92	0	0.53	40.29	66.37	2.87
iron trap	0	30.72	138.12	1.55	1.57	81.87	113.99	11.59
				Mol (%)				
control trap								
Nsats	0	19.29	22.03	0	66.67	20.86	2.52	36.38
MBSats	0	0	0.71	0	0	0.42	0.73	0
TBSats	0	7.31	8.0	0	0	7.67	11.78	8.45
Bmonos	0	0	0.38	0	0	0.98	1.03	0
Monos	0	73.39	68.86	0	33.33	69.87	83.83	55.17
iron trap								
Nsats	0	21.42	20.18	44.70	63.76	19.96	22.40	29.21
MBSats	0	0	0.53	0	7.44	0.53	0.56	1.30
TBSats	0	10.23	11.35	0	0	10.47	11.30	9.63
Bmonos	0	0	0.56	0	0	1.07	0.87	0.64
Monos	0	68.36	67.38	55.30	28.80	67.96	64.80	59.22

[a] Nsats, normal saturates; MBSats, midchain branched saturates; TBSats, terminally branched saturates; Bmonos, branched monounsaturates; Monos, monounsaturates.

tion detected in groundwater. The ability of denitrifying *Pseudomonas* to reduce soluble U(VI) is established (*42*), but the actual role of *Pseudomonas* sp. in this biostimulated uranium reduction remains unclear.

The ^{13}C enrichment was clearly detectable in PLFAs, especially with 16:1ω7c from samples in wells M-03 and M-08. However, due to an unexpected high labeling of fatty acids but total amounts of biomass near the quantification limits of the isotope ratio mass spectrometer (a factor of 5−10 less sensitive than the regular GC−MS) the exact isotopic shift, and therefore amount of labeled carbon incorporation, often could not be determined. Values for the isotopic shift are not given in this study as GC−IRMS analysis was unable to analyze suffient numbers of desired FAME peaks in the majority of samples. Larger traps or longer incubation times will be needed in the future.

Biomass and Community Structures. The microbial community changes were followed by down-well deployed bio-traps. The bacterial biomass (measured as pmole PLFA per bead) was determined as the total PLFA minus the normal saturates over 18 carbons in length and the polyenoic PLFA. Both of these are generally associated with eukaryote biomass (*29, 47*). The biomass content at the site also indicated a biostimulatory effect by acetate, showing considerable biomass in downgradient monitoring wells compared to background wells. The well M-08 exhibited the highest biomass among all four wells for both traps at both depths (Table 2), which coincided with the highest sulfate and uranium reduction observed in well M-08. This supports the hypothesis that the subsurface alterations are microbially driven and the rate of reduction is a function of microbial abundance. The iron traps exhibited a higher biomass compared to control traps. In agreement with the DNA analyses, minor differences were detected between control traps and iron traps at the respective wells, but they generally exhibited similar patterns.

PLFA analysis provided additional evidence in support of ^{13}C-DNA results by revealing the dominance of monounsaturated fatty acids (represented over 65% of the total PLFA) in downgradient monitoring wells compared with the background well (Table 2), which is indicative of a large population of Gram-negative bacteria within the community (*48*). An enrichment of terminally branched saturates (Table 2), indicating potential anaerobic sulfate-reducing bacteria (*49*), was consistently observed in downgradient monitoring wells M-03 and M-08. These two fatty acid groups represented the largest change in the microbial community structure upon acetate injection and are in general agreement with the ^{13}C-DNA results. Furthermore, quinone analysis of a *Geobacter sulfurreducens* culture indicated MK8 as a major quinone of this organism, comprising 89% of the total quinone measured (R. Geyer, unpublished results). Data from the bio-traps showed a steady increase of the relative abundance of MK8 in downgradient wells following acetate injection (Table 1). This steady production and accumulation in MK8 is highly consistent with the active *Geobacter* sequence dominance observed.

In all cases, labeling of active microbial populations was achieved by addition of an assimilable substrate. However, acetate may in principle be co-assimilated by other bacteria that are present and active in the same habitat but that utilize a different type of electron acceptor. The use of additional methods, such as PLFA and quinone ratios, is important in ensuring the quality of results.

Method Evaluation. Molecular techniques for analyzing bacterial community structure allow monitoring of changes in structure and function of bacterial assemblages during acetate biostimulation. However, studies of microbial communities have typically focused either on their structures or their metabolic functions. Linking structure and function remains a challenge, particularly at the field scale. The current research, combining geochemical analyses and ^{13}C amended Bio-Sep beads as in situ biofilm samplers (bio-traps), proved to be successful in this aspect and provided a practical and promising strategy to link microbial function to microbial identity at the field scale.

The acetate injected at the field contained no isotopic label, while the Bio-Sep beads bio-traps carried ^{13}C carbons. The beads amended with ^{13}C-acetate selectively labeled biomarkers in colonizing organisms involved in acetate metabolism, including those that appeared to be involved in U reduction, with subsequent recycling of labeled biomass. Thus, the active populations incorporating isotopic labels can be evaluated by examining the bio-films formed on Bio-Sep beads. The advantage of working with the ^{13}C amended Bio-Sep beads is the relatively high abundance of biomass that could be recovered, and the ease of ^{13}C application at the point of interest. By incorporating the amendments into Bio-Sep beads, the resulted bio-traps can serve as slow-release isotope sources when incubated in the aquifer. All of which renders the strategy low cost and easy to handle, making it feasible for field-scale application. Other amendments can

be fabricated into the beads for a variety of different research purposes.

Acknowledgments

The work was supported by the U.S. Department of Energy, Office of Science; grant DE-FC02-96ER62278 to D.C.W. as part of the Assessment Component of the Natural and Accelerated Bioremediation Research Program (NABIR), administered under Biological and Environmental Research, Environmental and Remediation Sciences Division of the U.S. Department of Energy, Office of Science. Support for the field experiment, field sampling, field data collection, and geochemical analyses was also provided by NABIR to Pacific Northwest National Laboratory and the University of Massachusetts. Pacific Northwest National Laboratory is managed by Battelle Memorial Institute for the United States Department of Energy under Contract DE-AC06-76RL01830.

Supporting Information Available

Layout of the biostimulation test site and leverage plots of correlation between redox potential and sulfate concentration. This material is available free of charge via the Internet at http://pubs.acs.org.

Literature Cited

(1) Ludwig, W.; Schleifer, K. H. Bacterial phylogeny based on 16S and 23S rRNA sequence analysis. *FEMS Microbiol. Rev.* **1994**, *15*, 155−73.

(2) Owen, R. J. Bacterial taxonomics: finding the wood through the phylogenetic trees. *Methods Mol. Biol.* **2004**, *266*, 353−83.

(3) White, D. C.; Ringelberg, D. B. Signature Lipid Biomarker Analysis. In *Techniques in Microbial Ecology*; Oxford University Press: New York, 1998.

(4) Findlay, R. H.; Pollard, P. C.; Moriarty, D. J.; White, D. C. Quantitative determination of microbial activity and community nutritional status in estuarine sediments: evidence for a disturbance artifact. *Can. J. Microbiol.* **1985**, *31*, 493−8.

(5) Frostegård, Å.; Tunlid, A.; Bååth, E. Changes in microbial community structure during long-term incubation in two soils experimentally contaminated with metals. *Soil Biol. Biochem.* **1996**, *28*, 55−63.

(6) Radajewski, S.; Ineson, P.; Parekh, N. R.; Murrell, J. C. Stable-isotope probing as a tool in microbial ecology. *Nature* **2000**, *403*, 646−9.

(7) Radajewski, S.; McDonald, I. R.; Murrell, J. C. Stable-isotope probing of nucleic acids: a window to the function of uncultured microorganisms. *Curr. Opin. Biotechnol.* **2003**, *14*, 296−302.

(8) Fang, J.; Lovanh, N.; Alvarez, P. J. The use of isotopic and lipid analysis techniques linking toluene degradation to specific microorganisms: applications and limitations. *Water Res.* **2004**, *38*, 2529−36.

(9) Hanson, J. R.; Macalady, J. L.; Harris, D.; Scow, K. M. Linking toluene degradation with specific microbial populations in soil. *Appl. Environ. Microbiol.* **1999**, *65*, 5403−8.

(10) Arao, T. In situ detection of changes in soil bacterial and fungal activities by measuring ^{13}C incorporation into soil phospholipid fatty acids from ^{13}C acetate. *Soil Biol. Biochem.* **1999**, *31*, 1015−20.

(11) Geyer, R.; Peacock, A. D. et al. In situ assessment of microbial activity using microcosms loaded with ^{13}C-labeled benzene or toluene. *Environ. Sci. Technol.* **2005**, *39*, 4983−4989.

(12) Peacock, A. D.; Chang, Y. J.; Istok, J. D.; Krumholz, L.; Geyer, R.; Kinsall, B.; Watson, D.; Sublette, K. L.; White, D. C. Utilization of Microbial Biofilms as Monitors of Bioremediation. *Microb. Ecol.* **2003**, *47*, 284−92.

(13) Sublette, K. L.; Peacock, A. D.; Davis, G. A.; Harrison, M. C.; Geyer, R.; White, D. C. In Situ Monitoring of the Remediation of Chlorinated Hydrocarbons Using "Bug Traps". In *Proceedings of the 7th International Symposium on In Situ and On-Site Bioremediation*, Orlando, FL; Battelle Press: Columbus, OH; 2003.

(14) Lloyd, J. R.; Lovley, D. R. Microbial detoxification of metals and radionuclides. *Curr. Opin. Biotechnol.* **2001**, *12*, 248−53.

(15) Lovley, D. R. Fe(III) and Mn(IV) reduction. *Environ. Microbe−Met. Interact.* **2000**, 3−29.

(16) Abdelouas, A.; Lutze, W.; Gong, W.; Nuttall, H. E.; Strietelmeier, B. A.; Travis, B. J. Biological reduction of uranium in groundwater and subsurface soil. *Sci. Total Environ.* **2000**, *250*, 21−35.

(17) Anderson, R. T.; Vrionis,H. A.; Ortiz-Bernard, I.; Resch, C. T.; Long, P. E.; Dayvault, R.; Karp, K.; Marutzky, S.; Metzler, D. R.; Peacock, A.; White, D. C.; Lowe, M.; Lovley, D. R. Stimulating the in situ activity of *Geobacter* species to remove uranium from the groundwater of a uranium-contaminated aquifer. *Appl. Environ. Microbiol.* **2003**, *69*, 5884−5891.

(18) Istok, J. D.; Senko, J. M.; Krumholz, L. R.; Watson, D.; Bogle, M. A.; Peacock, A.; Chang, Y. J.; White, D. C. In situ bioreduction of technetium and uranium in a nitrate-contaminated aquifer. *Environ. Sci. Technol.* **2004**, *38*, 468−75.

(19) U.S. Department of Energy. *The UMTRA Project Old Rifle Site*; GJO-99-88-TAR; U.S. Governement Printing Office: Washington, DC, 1999.

(20) McKinley, J. P.; Stevens, T. O.; Fredrickson, J. K.; Zachara, J. M.; Colwell, F. S.; Wagnon, K. B.; Smith, S. C.; Rawson, S. A.; Bjornstad, B. N. Biogeochemistry of anaerobic lacustrine and paleosol sediments within an aerobic unconfined aquifer. *Geomicrobiol. J.* **1997**, *14*, 23−39.

(21) McKinley, J. P.; Zachara, J. M.; Smith, S. C.; Turner, G. D. The influence of uranyl hydrolysis and multiple site-binding reactions on adsorption of U(VI) to montmorillonite. *Clays Clay Miner.* **1995**, *43*, 586−98.

(22) Chang, Y. J. Ph.D. Thesis. The University of Tennessee, Knoxville, TN, 2005.

(23) Muyzer, G.; de Waal, E. C.; Uitterlinden, A. G. Profiling of complex microbial populations by denaturing gradient gel electrophoresis analysis of polymerase chain reaction-amplified genes coding for 16S rRNA. *Appl. Environ. Microbiol.* **1993**, *59*, 695−700.

(24) Chang, Y. J.; Stephen, J. R.; Richter, A. P.; Venosa, A. D.; Bruggemann, J.; Macnaughton, S. J.; Kowalchuk, G. A.; Haines, J. R.; Kline, E.; White, D. C. Phylogenetic analysis of aerobic freshwater and marine enrichment cultures efficient in hydrocarbon degradation: effect of profiling method. *J. Microbiol. Methods* **1999**, *40*, 19−31.

(25) Gilbert, D. G. *SeqPup*. Department of Biology, Indiana University, Bloomington, Indiana, IN 47405, 1996**.**

(26) Maidak, B. L.; Cole, J. R.; Parker, C. T., Jr.; Garrity, G. M.; Larsen, N.; Li, B.; Lilburn, T. G.; McCaughey, M. J.; Olsen, G. J.; Overbeek, R.; Pramanik, S.; Schmidt, T. M.; Tiedje, J. M.; Woese, C. R. A new version of the RDP (Ribosomal Database Project). *Nucleic Acids Res.* **1999**, *27*, 171−3.

(27) Strunk, O.; Ludwig. W. ARB, Technical of University of Munich, Munich, Germany. 1997.

(28) Bligh, E. G.; Dyer, W. J. A rapid method of total lipid extraction and purification. *Can. J. Biochem. Physiol.* **1954**, *37*, 911−7.

(29) White, D. C.; Bobbie, R. J.; Heron, J. S.; King, J. D.; Morrison, S. J. In *Native Aquatic Bacteria: Enumeration, Activity, and Ecology*; Costerton, J. W. , Colwell, R. R., Eds; ASTM STP 695; American Society for Testing and Materials: Philadelphia, PA, 1979; pp 69−81.

(30) Mayberry, W. R.; Lane, J. R. Sequential alkaline saponification/acid hydrolysis/esterifiation: a one tube method with enhanced recovery of both cyclopropane and hydroxylated fatty acids. *J. Microbiol. Methods* **1993**, *18*, 21−32.

(31) Geyer, R.; Peacock, A. D.; White, D. C.; Lytle, C.; Van Berkel, G. J. Atmospheric Pressure Chemical Ionization and Atmospheric Pressure Photoionization for Simultaneous Mass Spectrometric Analysis of Microbial Respiratory Ubiquinones and Menaquinones. *J. Mass Spectrom.* **2004**, *39*, 922−29.

(32) Lensing, H. J.; Vogt, M.; Herrling, B. Modeling of biologically mediated redox processes in the subsurface. *J. Hydrol.* **1994**, *159*, 125−43.

(33) Polglase, W. J.; Pun, W. T.; Withaar, J. Lipoquinones of *Escherichia coli*. *Biochim. Biophys. Acta* **1966**, *118*, 425−6.

(34) Collins, M. D.; Jones, D. Distribution of isoprenoid quinone structural types in bacteria and their taxonomic implications. *Microbiol. Rev.* **1981**, *45*, 316−54.

(35) Hiraishi, A. Isoprenoid Quinones as Biomarkers of Microbial Populations in the Environment. *J. Biosci. Bioeng.* **1999**, *83*, 449−60.

(36) Kauffman, J. W.; Laughlin, W. C.; Baldwin, R. A. Microbiological treatment of uranium mine waters. *Environ. Sci. Technol.* **1986**, *20*, 243−8.

(37) Liger, E.; Charlet, L.; van Cappellen, P. Surface catalysis of uranium(VI) reduction by iron(II). *Geochim. Cosmochim. Acta* **1999**, *63* 2939−55.

(38) Coleman, M. L.; Hedrick, D. B.; Lovley, D. R.; White, D. C.; Pye, K. Reduction of Fe(III) in sediments by sulfate-reducing bacteria. *Nature* **1993**, *361*, 436−8.

(39) Lovley, D. R.; Phillips, E. J. Reduction of uranium by *Desulfovibrio desulfuricans*. *Appl. Environ. Microbiol.* **1992**, *58*, 850−6.
(40) Lovley, D. R.; Roden, E. E.; Phillips, E. J. P.; Woodward, J. C. Enzymatic iron and uranium reduction by sulfate-reducing bacteria. *Mar. Geol.* **1993**, *113*, 41−53.
(41) Tebo, B. M.; Obraztsova, A. Y. Sulfate-reducing bacterium grows with Cr(VI), U(VI), Mn(IV), and Fe(III) as electron acceptors. *FEMS Microbiol. Lett.* **1998**, *162*, 193−8.
(42) Barton, L. L.; Choudhury, K.; Thomson, B. M.; Steenhoudt, K.; Groffman, A. R. Bacterial reduction of soluble uranium: the first step of in situ immobilization of uranium. *Radioact. Waste Manage. Environ. Restor.* **1996**, *20*, 141−51.
(43) Spear, J. R.; Figueroa, L. A.; Honeyman, B. D. Modeling reduction of uranium U(VI) under variable sulfate concentrations by sulfate-reducing bacteria. *Appl. Environ. Microbiol.* **2000**, *66*, 3711−21.
(44) Petrie, L.; North, N. N.; Dollhopf, S. L.; Balkwill, D. L.; Kostka, J. E. Enumeration and characterization of iron(III)-reducing microbial communities from acidic subsurface sediments contaminated with uranium(VI). *Appl. Environ. Microbiol.* **2003**, *69*, 7467−79.
(45) Hansen, T. A. Carbon metabolism of sulfate-reducing bacteria. In *The Sulfate-Reducing Bacteria: Contemporary Perspectives*; Odom, J. M., Singleton, R., Jr., Eds.; Springer: New York, 1993; pp 21−40.
(46) Betlach, M. R. Evolution of bacterial denitrification and denitrifier diversity. *Antonie Van Leeuwenhoek* **1982**, *48*, 585−607.
(47) Bossio, D. A.; Scow, K. M. Impacts of Carbon and Flooding on Soil Microbial Communities: Phospholipid Fatty Acid Profiles and Substrate Utilization Patterns. *Microb. Ecol.* **1998**, *35*, 265−73.
(48) Wilkinson, S. G. In *Microbial Lipids*; Ratledge, C., Wilkinson, S. G.; Academic Press: London, 1988; pp 299−488.
(49) Dowling, N. J. E.; Widdel, F.; White, D. C. Phospholipid ester-linked fatty acid biomarkers of acetate-oxidizing sulfate-reducers and other sulfide forming bacteria. *J. Gen. Microbiol.* **1986**, *132*, 1815−25.

Received for review June 26, 2005. Revised manuscript received September 13, 2005. Accepted September 14, 2005.

ES051218U